Model test study of zonal disintegration phenomenon (ZDP) in deep rock mass under hydrostatic pressure

Qiang Gao[1,*], Qiangyong Zhang[1], Wen Xiang[1] and Xutao Zhang[2]

[1]Geotechnical and Structural Engineering Research Center, Shandong University, Jinan, China
[2]School of Architecture and Engineering, Liaocheng University, Liaocheng, China

*Corresponding author e-mail: gaoqiangsdu@163.com

Abstract. The zonal disintegration phenomena (ZDP) will appear with the increasing of the depth of underground engineering which are different from shallow tunnel. In order to investigate the formation mechanism and influence factor of ZDP, taking the deep tunnel of Dingji coal mine with high geostress as background, the true 3D geomechanical model tests under hydrostatic pressure have been carried out by adopting model similar materials and numerical controlling true 3D loading model test system. The model test results show that: (1) Only when the geostress satisfies certain stress conditions, the ZDP will appear under hydrostatic pressure. (2) Geostress is an important influence factor for ZDP of rock mass under hydrostatic pressure. The radial displacements of surrounding rock increase obviously because of high geostress. The higher value of geostress is, the larger range of fractured zone is. (3) The changing laws of displacements of the surrounding rocks by means of advanced and exact measurement method are obtained. The results of displacements and the distribution of fractured areas are basically consistent. The model test results help to reveal the influence factor of ZDP, which lays a solid test foundation for further studying nonlinear deformation characteristics and failure mechanism of deep rock mass.

1. Introduction

The zonal disintegration phenomenon (ZDP) is one of the unique destruction phenomena that occurred during the excavation of deep rock masses [1]. During the excavation process of many deep tunnel projects at home and abroad, the existence of ZDP was confirmed through various physical detection methods [2-4]. Some geotechnical model tests were made and a common conclusion was put forward: the ZDP is going to happen when the maximum principal stress is parallel to the tunnel axis and exceeds a certain value [5-7].

Meanwhile, some experts point out the following points that the stress state of the deep rock mass tends to hydrostatic pressure with the increasing depth and $\sigma_1 = \sigma_2 = \sigma_3$ is used as a criterion for determining the deep mining depth [8, 9]. Gaze AM [10] believe that the deep rock masses in the deep internal space has been transformed into a non-Euclidean geometric space because of the development of joints and fissures, the non-monotonic variation law of the stress of the surrounding rock under the condition of hydrostatic pressure is found and the mechanism of the ZDP is analyzed by adopting the non-Euclidean geometry theory. According to the non-Euclidean geometric model, the zonal

Content from this work may be used under the terms of the Creative Commons Attribution 3.0 licence. Any further distribution of this work must maintain attribution to the author(s) and the title of the work, journal citation and DOI.
Published under licence by IOP Publishing Ltd

disintegration distribution law of deep-damaged surrounding rock under the conditions of hydrostatic pressure is obtained [11-12]. The above scholars analyzed the ZDP under hydrostatic pressure through theoretical analysis, but failed to obtain relevant test verification from the model test.

Therefore, taking the deep tunnel of Dinghy coal mine in Huainan mining area as the engineering background, the ZDP of deep rock mass under the hydrostatic pressure is present by 3D geotechnical model test, and valuable experimental reference for revealing the ZDP fractured model is provided.

2. Geotechnical Model Test

2.1. Similar materials of model test

The deep tunnel of the Dinghy coal mine is chosen as the engineering prototype of the model test, the geometrical similarity scale of the model is taken as 50 and the similar weight ratio of the model is taken as 1. Based on the similarity principle and the mechanical parameters of the rock, rock materials were simulated using new typed cementations geotechnical similar material for iron crystal sand [13]. Through a large number of material ratios and corresponding mechanical parameter tests, the physical and mechanical parameters of similar materials of the model were measured and obtained in Table 1.

Table 1. Physical and mechanical parameters of prototype rock and model material

Material type	Unit weight (kN • m-3)	Deformation modulus (MPa)	Cohesion (MPa)	Friction angle (°)	Compression strength (MPa)	Poisson ratio
Prototype material	26.2	12970	10.00	43	88.55	0.268
Model material	25.9-26.5	251-270	0.18-0.22	40-45	1.70-1.90	0.24-0.28

2.2. Model test working conditions

The true three-dimensional geomechanical model tests were carried out under three different stress loading conditions. The test conditions are detailed in Figure 1.

The simulated dimensions of the geomechanical model are: length (direction of parallel tunnel axis, x direction) × width (direction of vertical tunnel axis, y direction) × height (vertical direction, z direction) = 0.6m × 0.6m × 0.6 m. The model tunnels in three working conditions are all excavated using circular holes. The diameter of the hole is 0.1m.

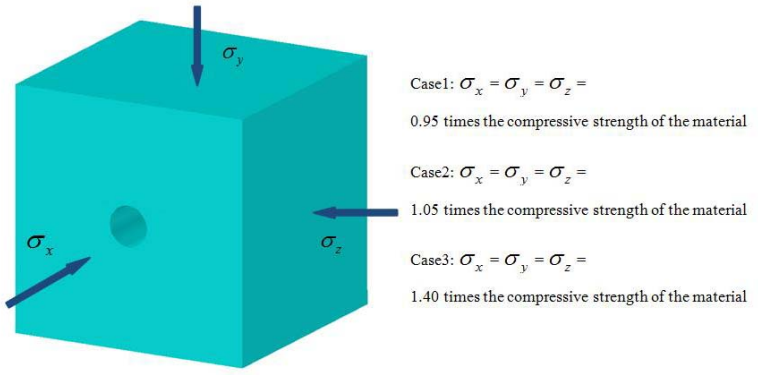


Figure 1. Model test working conditions and loading mode

2.3. Manufacture method of geomechanical model

The geomechanical model was produced using a layered compaction and air-drying method [14]. The basic flow is shown in Figure 2. In order to avoid the formation of layers in the model, the surface of

the upper layer material must be roughened and moistened with alcohol before the next layer of material is filled.

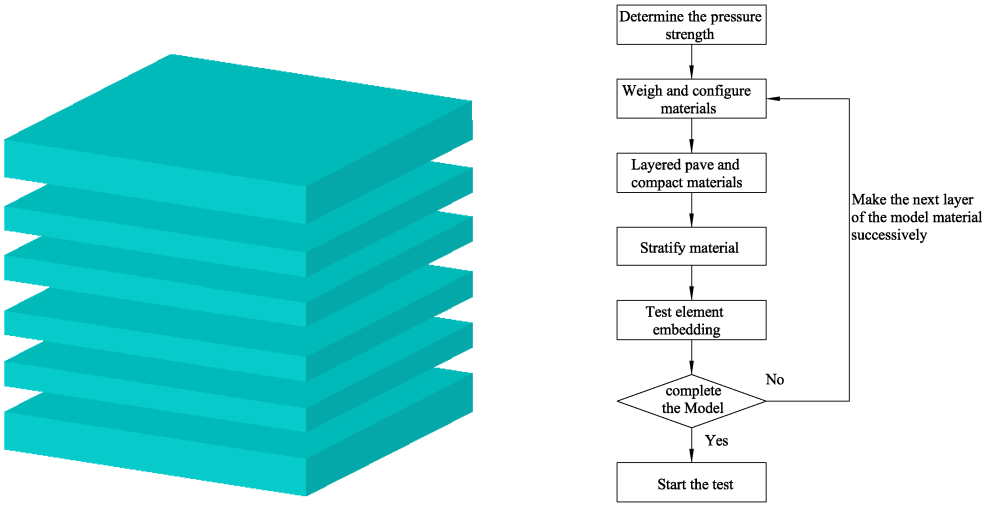


Figure 2. The flow chart of tunnel model

2.4. Arrangement of model measuring elements

In order to effectively observe the ZDP of tunnel surrounding rock, the high-precision multi-point displacement meter are embedded in the model area. The layout of the model monitoring section and the arrangement of the measuring components are shown in Figure 3.

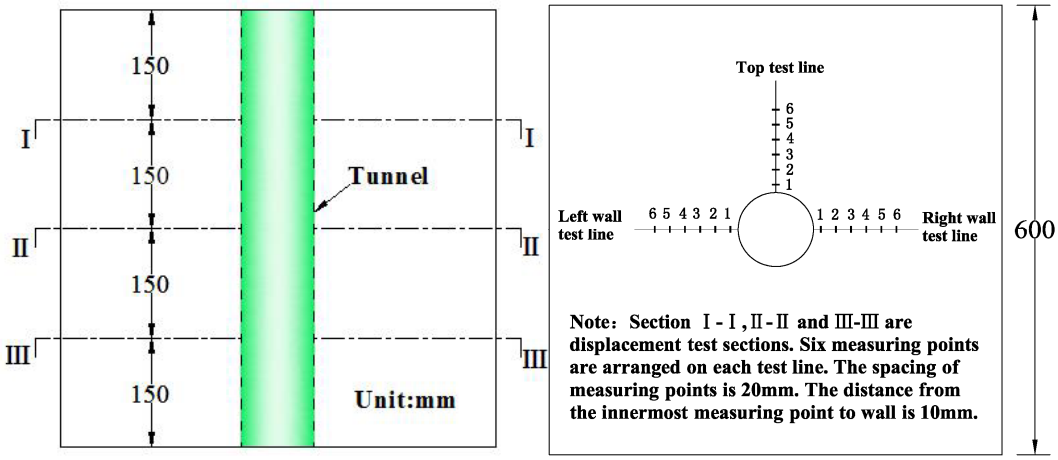


Figure 3. Layout scheme of model monitoring sections

2.5. Model Loading and Excavation

According to the loading method described in Section 2.2, a self-designed high-stress true three-dimensional loading model test system [7] is used to apply boundary load to the model so that the initial stress field is formed inside the model. The model boundary loading should be increased proportionately to a predetermined level. The value should be kept unchanged after the completion of the loading. After a long period of stabilization, the excavation of the model tunnel is performed.

The model excavation adopts the artificial drilling and excavation method of the full tunnel section, the excavation footage is 50mm (corresponding to the 2.5m of prototype), and the excavation is paused once the excavation of one footage is completed, the excavation time is recorded, and the reading of the monitoring instrument is stable. Then proceed with the excavation and test recording of

the next footage until the completion of the excavation of the tunnel. Figure 4 shows a photograph of the model tunnel excavating and testing.



Figure 4. Excavating and testing scheme of model tunnel

3. Geomechanical model test results and analysis

3.1. Contrastive Analysis of Destruction of tunnel

After the tunnel excavation is completed, the boundary stress is to be maintained for a long time. When the reading of the monitoring instrument is stabilized, the boundary stress is removed and the model test bench is disassembled, the geomechanical models under three kinds of test conditions are sliced along the direction of the tunnel axis and observed the following phenomena which are seen in Figure 5.



(a)Case 1 (b) Case 2 (c) Case 3

Figure 5. The ZDP in the model tunnel

Form the Figure 5 (a) and (b), we can see that only when the eustress satisfies certain stress conditions, that is the eustress is greater than the rock compressive strength, the ZDP will appear under hydrostatic pressure.

The damage conditions of the model tunnel are listed in Table 2. For the actual measurement of the number of layers and scope of the fractured zones under three kinds of test conditions, we find that the surrounding rock within the range of 1~2cm of the model tunnel is seriously damaged and the phenomenon of serious collapse was occurred during the excavation process, and it can be considered as a traditional rock loose circle. In case 2 and 3, the subsequent fractured zones and non-fractured zones are arranged at intervals and in a loop-like state, which is a typical ZDP.

Taking the tunnel center as the measurement starting point, the scope of the fractured area is analyzed. The average radius and average width of each fractured zone are shown in Table 2.

Table 2. Average radius and average width of fractured zones in model test

Fractured area number	Case 1		Case 2		Case 3	
	Average radius (cm)	Average width (cm)	Average radius (cm)	Average width (cm)	Average radius (cm)	Average width (cm)
1	5.45	0.45	6.25	1.25	6.40	1.40
2			8.45	1.10	8.65	0.90
3			9.80	0.60	10.05	0.70
4			11.25	0.30	11.40	0.50
5					12.55	0.30
6					13.90	0.20

The comparative analysis of the damage situation of the model tunnel are shown that: in case 1, the number of the fractured zones is 1 layer, that means there is no ZDP emerged in such eustress condition, the maximum radius of the fractured zone is 1.09 times the radius of the tunnel. In case 2 and 3, the number of the fractured zones is 4 layers and 6 layers respectively that means the ZDP appear in such geostress condition, the maximum radius of the fractured zone is 2.25 and 2.78 times the radius of the tunnel, respectively. The comparison is shown in Figure 6.

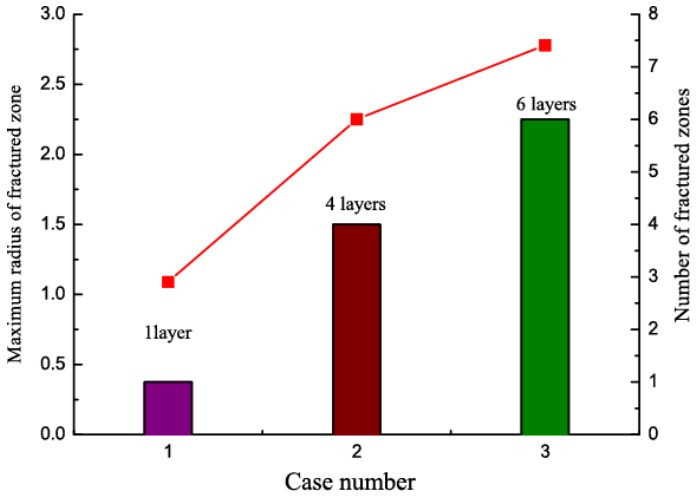


Figure 6. Contrast of number and maximum radius of fractured zones

Under different test conditions

3.2. The change law of each measured point value around the tunnel

During the excavation process of the model tunnel, the high-precision multi-point displacement measurement system is used to monitor and record the radial displacement of the model. The radial displacement of each measurement point under the three test conditions is listed in the Table 3. The radial displacement direction is pointed to the interior of the tunnel, and the data have been converted to the displacement value of the prototype.

Table 3. Radial displacements of model tunnel

Test conditions and test sections		Case 1	Case 2	Case 3
Top wall measuring point radial displacement (mm)	1	30.35	64.85	73.55
	2	20.25	39.85	46.50
	3	18.55	53.70	62.55
	4	12.8	46.50	54.55
	5	6.45	38.35	44.75
	6	5.6	18.45	28.70
Left measuring point radial displacement (mm)	1	27.50	44.05	63.10
	2	16.25	38.90	45.50
	3	10.40	50.45	59.25
	4	7.25	34.95	40.90
	5	4.35	36.35	42.15
	6	2.35	9.30	13.65
Right wall measuring point radial displacement (mm)	1	28.85	55.75	60.55
	2	16.05	42.50	49.30
	3	8.45	56.05	65.15
	4	5.60	36.75	42.35
	5	4.15	41.35	48.15
	6	2.40	19.20	26.50

The radial displacements around the model tunnel are shown in Figure 7.

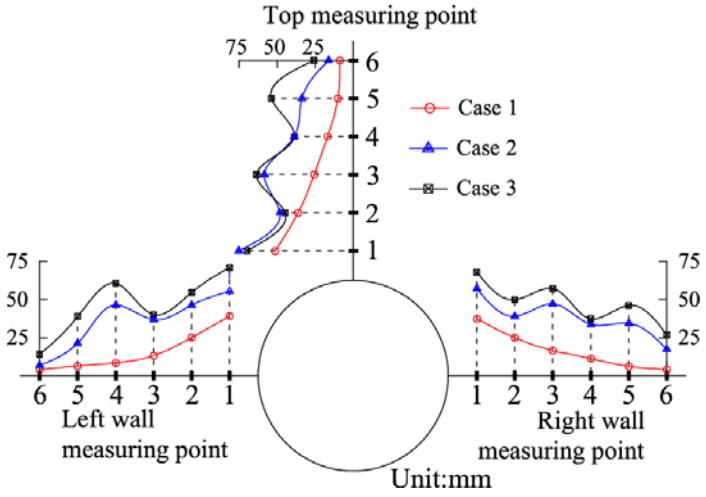


Figure 7. Radial displacements around the model tunnel

Under different test conditions

Comparative analysis of the radial displacement at each measurement point of the model tunnel under three kinds of test conditions are shown that:

In case 1, the radial displacements of the measured points around the model tunnel all show monotonically decreasing trend. In case 2 and 3, the radial displacements are showed the oscillated variation of peaks and troughs alternately.

(2) Comparing the magnitude law of radial displacement at the same position of the model tunnel in three kinds of test conditions, it is found that the case 3 is the largest while the case 1 is the smallest. This shows that under certain geostress conditions, the higher the geostress is, the more easily the ZDP

occurs, and the more layer number of the fractured zones around the tunnel is, and the larger range of fractured zones is.

Taking case 2 as an example, because of the high geostress, the surrounding rock stress is released after excavation. With the process of tunnel excavation under high hydrostatic pressure, the higher tensile strain appears in surrounding rock because of the emerging of tunnel free surface, then the tensile failure occurs in surrounding rock. Due to the high geostress, there is still a large range of surrounding rock in the post-peak strain softening stage outside the tensile failure zone. In this range, the displacement of surrounding rock shows the oscillation law, in which the wave peak and wave trough appear alternately. It is precisely because of the oscillation law, the discontinuous localization failure zones appear in the surrounding rock. In the fractured zone of surrounding rock, the radial displacement is wave peak value. However, in the middle of the two adjacent failure zones, the radial displacement of surrounding rock is wave trough value (Figure 8). The oscillation law of displacement in deep surrounding rock is the key reason of zonal disintegration.

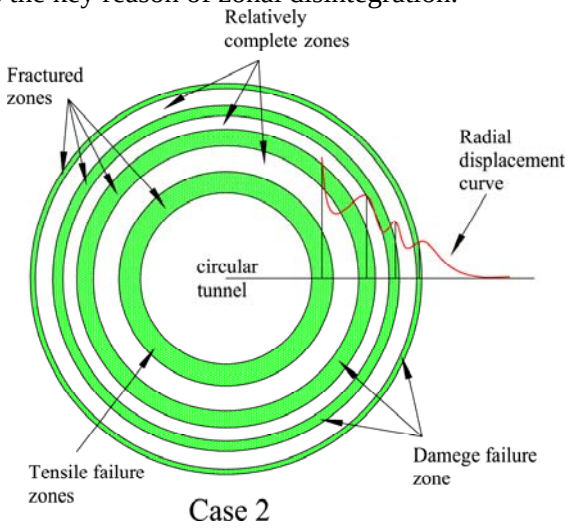


Figure 8. Mechanism of zonal disintegration in deep tunnel.

4. Conclusion

In order to investigate the formation mechanism and influence factor of ZDP, taking the deep tunnel of Dingji coal mine in Huainan mining area as the engineering background, the true 3D geomechanical model tests under different hydrostatic pressure have been carried out by adopting model similar material and numerical controlling true 3D loading model test system. The high-precision multi-point displacement measurement system is monitored and recorded the radial displacement changes around the model tunnel. The following conclusions were obtained:

Based on the condition of satisfying certain geostress, that is the geostress is greater than the rock compressive strength, the ZDP will occur under hydrostatic pressure.

Under the same physical and mechanical parameters, the radial displacements of surrounding rock increase obviously because of high hydrostatic pressure. The higher hydrostatic pressure is, the larger range of fractured zone is, and the more obviously the ZDP occurs.

The results of displacements and the distribution of fractured areas are basically consistent, and the oscillation law of displacement in deep surrounding rock is the key reason of zonal disintegration.

Acknowledgments

This work was financially supported by the National Key Research and Development Program of China (No. 2016YFC0401804-03), the Project of Taishan scholar Engineering, the National Natural Science Foundation of China (No. 41772282), the Preliminary Research Project of the Underground Experimental Project for the Geological Disposal of High-level Radioactive Waste (No. YKKY-J-2015-25). The authors are deeply grateful for the support.

References

[1] QIAN Qihu. The character scientific phenomena of engineering response to deep rock mass and the implication of deepness[J]. Journal of East China Institute of Technology, 2004, 27(1): 1-5.
[2] SHEMYAKIN E I, FISENKO G L, KURLENYA M V, et al. Zonal disintegration of rocks around underground workings, part I: data of in-situ observations[J]. Journal of Mining Science, 1986, 22(3): 157-168.
[3] ADAMS G D, JAGER A J. Petroscopic observations of rock fracturing ahead of the stope faces in deep-level gold mines[J]. Journal of the South Africa Institute of Mining and Metallurgy, 1980, (2): 115-127.
[4] LI Shucai ,WANG Hanpeng, QIAN Qihu, et al. In-situ monitoring research on zonal disintegration of surrounding rock mass in deep mine roadways[J]. Chinese Journal of Rock Mechanics and Engineering, 2008, 27(8): 1545-1553.
[5] GU Jincai, GU Leiyu, CHEN Anmin. Model test study on mechanism of layered fracture within surrounding rock of tunnels in deep stratum[J]. Chinese Journal of Rock Mechanics and Engineering, 2008, 27(3): 433-438.
[6] Zhang Q, Chen X, Lin B, et al. Study of 3D geomechanical model test of zonal disintegration of surrounding rock of deep tunnel[J]. Chinese Journal of Rock Mechanics and Engineering, 2009,28(09): 1757-1766.
[7] Zhang Q Y, Zhang X T, Xiang W, et al. Model test study of zonal disintegration in deep rock mass under different cavern shapes and loading conditions[J]. Chinese Journal of Rock Mechanics and Engineering, 2013, 32(8): 1564-1571.
[8] XIE Heping,GAO Feng,JU Yang. Research and development of rock mechanics in deep ground engineering[J]. Chinese Journal of Rock Mechanics and Engineering,2015,34(11):2161-2178.
[9] HAN Jun,ZHANG Hongwei,SONG Weihua,et al. In-situ stress field of coal and gas outburst mining area[J].Chinese Journal of Rock Mechanics and Engineering,2008,27(Supp.2):3852-3859.
[10] Guzev A M, Paroshin A A. Non-euclidean model of the zonal disinte- gration of rocks around an underground Working [J].Journal of Applied Mechanics and Technical Physics,2001,42 (1): 131-139.
[11] Xiaoping Zhou, Min Zhou, Qihu Qian. Influence of rock damage on zonal disintegration around deep circle tunnels [J]. Chinese Journal of Solid Mechanics, 2012, 33(3): 242-250.
[12] ZHOU Xiaoping,QIAN Qihu. Non-euclidean model of failure of deep rock masses under incompatible deformation[J]. Chinese Journal of Rock Mechanics and Engineering, 2013, 32(4): 767-774.
[13] ZHANG Qiangyong,LI Shucai,GUO Xiaohong. Research and development of new typed cementations geotechnical similar material for iron crystal sand and its application[J]. Rock and Soil Mechanics,2008,29(8): 2126–2130.
[14] ZHANG Qiang-yong, CHEN Xu-guang, LIN Bo. Study of 3d geomechanical model test of zonal disintegration of surrounding rock of deep tunnel[J]. Chinese Journal of Rock Mechanics and Engineering, 2009, 29(8): 1757-1766.